Numerical simulations of the Hall effect in inhomogeneous materials*

Itzhak Webman and Joshua Jortner
Department of Chemistry, Tel-Aviv University, Tel-Aviv, Israel

Morrel H. Cohen
The James Franck Institute, Department of Physics, The University of Chicago, Chicago, Illinois 60637
(Received 10 May 1976)

The Hall effect in microscopically inhomogeneous disordered materials was simulated by numerical calculations of the magnetoconductivity tensor in cubic resistor networks with correlated bonds. The numerical data were utilized for a quantitative fit of the Hall coefficient and the Hall mobility in metal-ammonia solutions and in alkali-tungsten bronzes.

I. INTRODUCTION

Hall-effect data in some disordered materials undergoing a metal-nonmetal transition have been of considerable importance in interpreting the electronic structure and transport properties in terms of a continuous transition via the inhomogeneous transport regime.[1-7] The effective-medium theory (EMT) generalized by Cohen and Jortner[8] for the Hall effect has been invoked for the analysis of the Hall data in a variety of microscopically inhomogeneous systems. A comparison of the EMT for the electrical conductivity with the results of numerical simulation on correlated resistor networks reveals that the EMT is valid for metallic volume fraction, C, well above the percolation threshold $C^* = 0.145 \pm 0.005$, and that the EMT is not reliable in the transition region for $C < 0.4$.[9,10] As a theoretical treatment of the magnetoconductivity tensor which goes beyond the EMT is not yet available, it is important to generalize the numerical simulation methods, previously applied for the conductivity,[9-12] to handle the case of a nondiagonal-magnetoconductivity tensor. In this paper we present such a generalized numerical simulation scheme for the Hall effect together with applications for some two-component microscopically inhomogeneous systems.

II. NUMERICAL SCHEME

We have recently shown[9,10] that numerical simulations of the conductivity in correlated resistor networks properly account for the continuous percolation problem in inhomogeneous materials characterized by a finite correlation length for the fluctuation in the state of the material. In the case of diagonal conductivity, the main effect of the correlations between bonds is to shift the percolation threshold from $C^* = 0.25$, the bond-percolation threshold in a cubic lattice, down to $C^* = 0.145 \pm 0.005$, the critical metallic volume fraction for percolation in a continuous system.[9,10] We shall now present an extended scheme for the numerical simulation of the magnetoconductivity tensor in correlated networks.

The numerical simulations of the magnetoconductivity tensor are based on a finite-difference solution of the continuity equation for an inhomogeneous medium;

$$\vec{\nabla} \cdot [\bar{\sigma}(\vec{r}) \cdot \vec{\nabla} \phi(\vec{r})] = 0, \tag{1}$$

where $\bar{\sigma}(\vec{r})$ is the conductivity tensor and $\phi(\vec{r})$ is the potential, both given at the point $\vec{r}$. The conductivity tensor will be written in the explicit form

$$\begin{pmatrix} g & h(H) & 0 \\ -h(H) & g & 0 \\ 0 & 0 & g \end{pmatrix}. \tag{2}$$

Each bond connecting the lattice sites $\vec{r}_i$ and $\vec{r}_j$ is assigned a pair of parameters g_{ij} and h_{ij} specifying the values of the diagonal and of the off-diagonal element of $\bar{\sigma}$ at the point $\frac{1}{2}(\vec{r}_i + \vec{r}_j)$ in the medium. For the case of a binary inhomogeneous medium, each bond is assigned either of the two pairs of values $g_{ij} = 1$ and $h_{ij} = h_0$, with probability C; $g_{ij} = x$ and $h_{ij} = h_0 xy$, with probability $1 - C$. x is the ratio of the conductivity at $C = 0$ to the conductivity at $C = 1$ and y is the ratio of the Hall mobility at $C = 0$ to the Hall mobility at $C = 1$. We chose $h_0 \ll 1$ to avoid magnetoresistance effects.

The finite-difference representation of Eq. (1), with $\bar{\sigma}$ given by Eq. (2), can be recast into the following generalized form of the Kirchoff vertex equation for a resistor network, which is displayed in Fig. 1;

$$\sum_{j=1}^{6} g_{0j}(\phi_j - \phi_0) + \sum_{j=1}^{4} (-1)^j h_{0j} E_{0j}^{\perp} = 0 \tag{3}$$

for the point $\vec{r}_0$, where $E_{0j}^{\perp}$ represents the component of the electrical field at $\frac{1}{2}(\vec{r}_0 + \vec{r}_j)$ perpen-

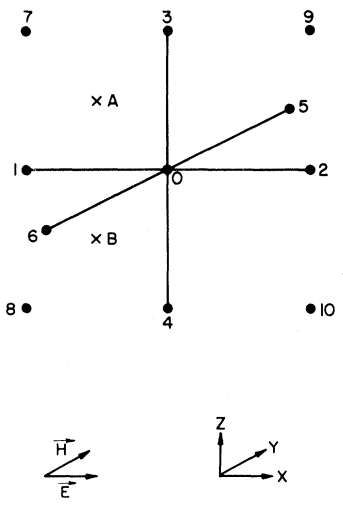

FIG. 1. Basic unit of the cubic lattice employed for solution of the finite difference representation, Eq. (2), of the continuity equation, Eq. (1).

dicular to both the bond $0j$ and to the magnetic field $\vec{H}$. $E_{0j}^{\perp}$ can be expressed in terms of the potentials at the nearest neighbors and the next-nearest neighbors of the site 0 (see Fig. 1), so that

$$E_{01}^{\perp} = \tfrac{1}{4}(\phi_7 - \phi_8 + \phi_3 - \phi_4). \tag{4}$$

Numerical simulations were carried out on correlated cubic networks which consist of regions of constant conductivity extending over several lattice distances. Since the transverse field $E_{0j}^{\perp}$ at a bond $0j$ is determined mainly by neighboring bonds which are orthogonal to it, these bonds must usually have the same conductivity value as the bond $0j$ except at the region boundaries. Correlations are therefore essential in the present case. The correlated networks were derived from a cubic network by means of a procedure which can be iterated to yield a sequence of progressively correlated networks.[10] The numerical calculations of conductivity on such networks[10] resulted in a series of functions $\sigma_n(x,C)$, where n is the order of correlation. We have found that $\sigma_n(x,C)$ converges rapidly to the limit $\sigma_\infty(x,C)$ and that $\sigma_5(x,C)$ provides an excellent approximation to σ in the large n limit. In the present work we have chosen $n=9$ as a representation of the continuous random medium. We have performed several calculations of the Hall coefficient and the Hall mobility for $n=4$ and $n=6$. While these transport properties were found to be more sensitive to the topology of the lattice and to the order of correlation than the conductivity, the results for $n=9$ was found to be very close (within 2%) to those for $n=6$. We conclude that convergence to the continuous percolation limit has been achieved at $n=9$. The sizes of cubic networks used for our numerical computations were $20\times20\times20$ and $30\times30\times30$. Boundary conditions in the y direction are cyclic, while in the z direction reflecting boundary conditions[13] were imposed in order to assure that no current flows out of the simulated sample in this direction. The Hall voltage was derived by averaging the potential difference between opposite sites on the xy faces of the lattice. The final Hall voltage was determined by taking the difference between the voltage evaluated with a finite magnetic field and that evaluated with the field switched off. Finally, the Hall mobility and the Hall coefficient are given by

$$\begin{aligned} &g(x,y,C)=\mu(x,y,C)/\mu_0 = V_H(x,y,C)/V_H(x,y,1),\\ &h(x,y,C)=R(x,y,C)/R_0 = g(x,y,C)/f(x,C), \qquad (5)\\ &f(x,C)=\sigma(x,C)/\sigma_0. \end{aligned}$$

σ_0, μ_0 and R_0 are the values of the electrical conductivity, Hall mobility, and Hall coefficient at $C=1$.

III. NUMERICAL RESULTS FOR THE HALL EFFECT

Plots of the Hall coefficient R for various values of x and y are presented in Fig. 2. A com-

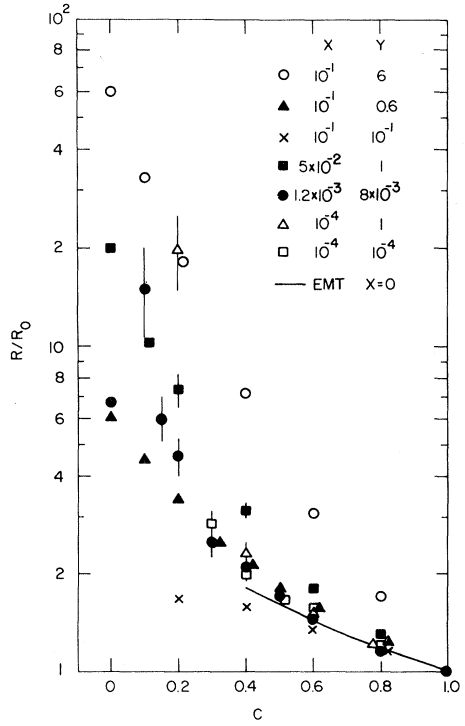

FIG. 2. Results of numerical simulation for the Hall coefficient of a two-component inhomogeneous medium.

parison of our numerical results for R with the EMT are presented in Fig. 3. The results for small values of $x \leq 10^{-2}$ are characterized by the following interesting features. First, $C \geq 0.4R$ is practically independent of y for small values of $x \leq 10^{-3}$. Second, for $C \geq 0.5$ the numerical results are in good agreement with the EMT for R for all values of x and y. For high values of both x and y, i.e., $x \geq 0.1$ and $y \geq 0.1$ the EMT[8] is adequate throughout the entire range, as expected. Third, just above the continuous percolation threshold $0.25 > C > C^*$, R exhibits a pronounced rise as $C \to C^*$. For high values of $x \geq 0.1$, $R(x, C)$ interpolates smoothly between $R(x, C = 1)$ and $R(x, C = 0)$.

Numerical data for the Hall mobility, together with the EMT results, are displayed in Fig. 4. We note that for high values of both x and y, i.e., $x > 0.05$ and $y \sim 1$, μ exhibits a weak dependence on C throughout the entire range. For $x = 0.05$ and $y = 1$, $\mu(C)$ varies only between 1.0 and 0.70, a change which is somewhat smaller than predicted by the EMT.[8] These numerical results are of interest for a quantitative determination of the Hall mobility in high-temperature inhomogeneous materials undergoing a metal-semiconductive transition, such as expanded liquid Hg,[2] and liquid Te.[6] Next, we also note that for low values of $x \leq 10^{-3}$ and for $C \geq 0.4$, μ is independent of y within the statistical spread of our numerical results.

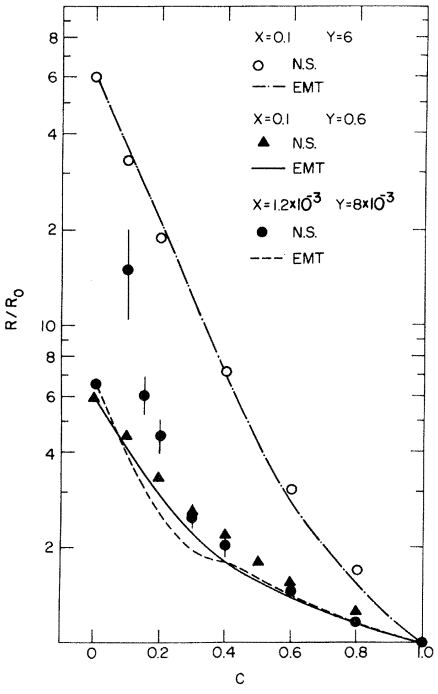

FIG. 3. Hall coefficient of an inhomogeneous medium evaluated by numerical simulation (NS) (dots) and by the effective-medium theory (EMT) (curves).

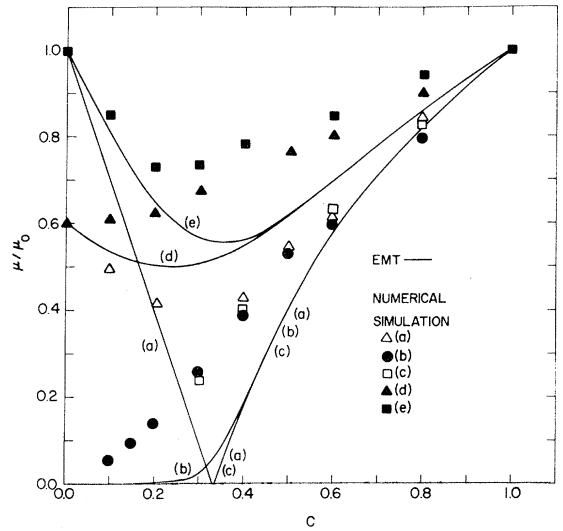

FIG. 4. Results of the numerical simulation (dots) and of the EMT (curves) for the Hall mobility of an inhomogeneous medium. (a) $x = 10^{-4}$, $y = 1$, (b) $x = 1.2 \times 10^{-3}$, $y = 8 \times 10^{-3}$, (c) $x = 10^{-4}$, $y = 10^{-4}$, (d) $x = 0.1$, $y = 0.6$, (e) $x = 1$, $y = 0.05$.

IV. ANALYSIS OF HALL DATA IN SOME MICROSCOPICALLY INHOMOGENEOUS MATERIALS

We now apply the data obtained herein from numerical simulations to (i) metal-ammonia solutions[14-16] and (ii) alkali-tungsten bronzes,[17] which undergo a continuous metal-nonmetal transition via the inhomogeneous-transport regime.

Jortner and Cohen[3] have recently proposed that in Li-NH_3 solutions the metallic propagation regime is separated from a nonmetallic regime by a microscopically inhomogeneous regime where the metal concentration fluctuates locally about either of two well-defined values M_0 and M_1, where $M_0 > M_1$, the local concentration remaining near M_0 or M_1 over radii which are approximately equal to the Debye short correlation length for concentration fluctuations. This physical picture is supported by concentration fluctuation determinations based on chemical potential measurements in Li and Na solutions,[18] and by small angle x-ray and neutron scattering[19,20] data in Li solutions. The limits of the inhomogeneous regime were determined by a combination of concentration fluctuation measurements, electrical conductivity, Hall effect and paramagnetic susceptibility data resulting in $M_0 = 9$ mole % metal and $M_1 = 2.3$ mole % metal for both Li-NH_3 at 223 K and Na-NH_3 at 240 K, resulting in the C scale, $C = \frac{1}{20}(3M - 7)$.[3] In Fig. 5 we have compared the experimental Hall effect data of Li-NH_3 solutions at 223 K,[21-24] with the results of the numerical simulations for $x = 1.2 \times 10^{-3}$ and $y = 8$

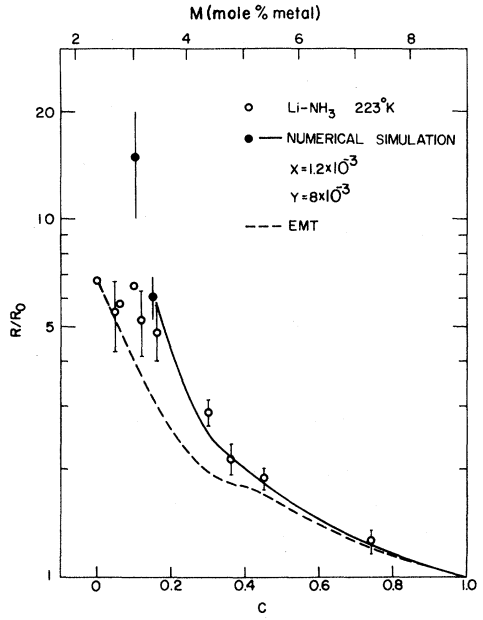

FIG. 5. Comparison of the results of numerical simulation (solid curve and full circles) and the EMT (dashed curve) with the Hall coefficient data of Li-NH_3 at 223 K.

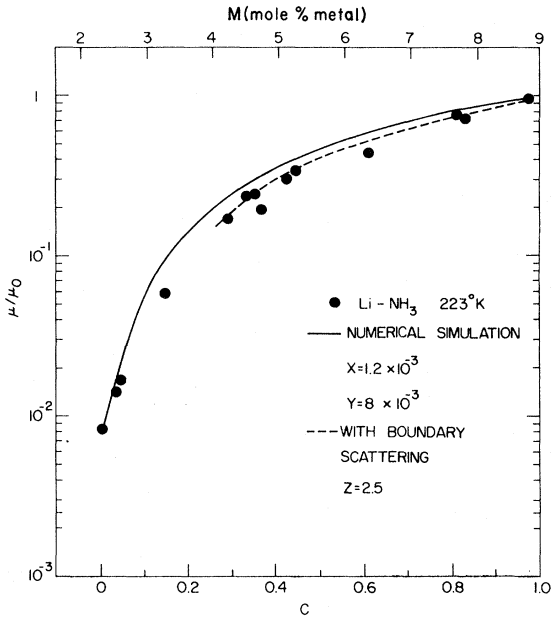

FIG. 6. Analysis of the Hall mobility data of Li-NH_3 at 223 K in terms of the results of numerical simulation (solid curve) and with boundary scattering corrections (dashed curve).

$\times 10^{-3}$. The fit of the numerical results for R to the experimental data is very good except at $C = 0.1$, where our numerical result for R is higher than the experimental result by a factor of ~ 2. At this low value of metallic-volume fraction, statistical fluctuations between numerical results calculated for different lattices are very pronounced, and averaging over a larger number of results may improve this fit. The calculated Hall mobility (Fig. 6) lies systematically above the experimental Hall-mobility data for Li-NH_3. This discrepancy results from the decrease in the local values of metallic conductivity with decreasing C due to scattering from region boundaries.[3-6] A similar effect is encountered in the case of electrical conductivity.[3] The Hall coefficient, however, is not as sensitive to boundary scattering, since $R = \mu/\sigma$, so that boundary-scattering corrections cancel out at least for $C \geq 0.4$. Boundary-scattering effects were accounted for with the parameter $z = 2b/l$, where b is the Debye correlation length and l is the mean free path. The fit of the experimental data with $z = 2.5$ becomes excellent. This value z was previously found to give the best fit of the experimental conductivity to the results of numerical simulations for σ for Li-NH_3 solutions.[3]

We have recently accounted for the electrical-transport properties of alkali-tungsten bronzes M_XWO_3,[7] in terms of a cluster model for the inhomogeneous medium consisting of metallic regions where the local metallic volume fraction is $X = 1$, and of semiconducting regions. Figure 7 displays the experimental R data[25-27] for alkali-tungsten bronzes at $T = 300$ K,[19] together with the

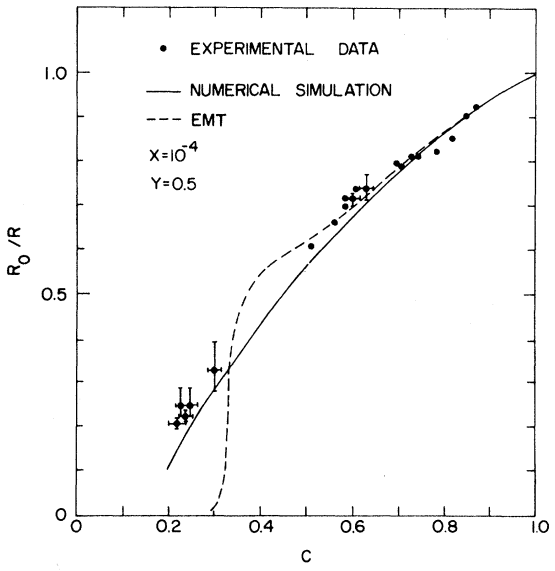

FIG. 7. Analysis of the Hall coefficient data of sodium tungsten bronzes at 300 K in terms of the results of numerical simulation (solid curve) and the EMT (dashed curve).

numerical results for $x = 10^{-4}$ and $y = 0.5$. The good fit of the available Hall data in the entire range $0.2 < C < 0.8$ and, in particular, in the range $C = 0.2$–0.3 where the EMT fails, provides additional support for the cluster model.

V. CONCLUDING COMMENTS

The numerical simulations of the magnetoconductivity tensor reported herein are useful for establishing the validity of the inhomogeneous-transport picture in some disordered materials. While this work is in progress Swenumson and Thompson[28] have performed numerical simulations of the Hall effect on $7 \times 7 \times 21$ networks. In their simulation algorithm they assign a conductivity tensor to groups of three orthogonal bonds at each site. Our studies of electrical conductivity show that the percolation threshold C^* is shifted from $C^* = 0.25$, for a noncorrelated network, down to $C^* = 0.15$, for a correlated network which simulates a continuous medium. We believe that for an accurate simulation of the Hall effect in a random medium by a finite-difference solution of Eq. (1), one should also have large zones of bonds possessing the same conductivity value. This is achieved by our correlation procedure. Another significant difference between our work and the work of Swenumson and Thompson is related to the choice of the transverse electrical field. While the longitudinal electric field $E_{01}^{\parallel}$ at a bond such as 01 (Fig. 1) is obviously given by $(\phi_1 - \phi_0)/\Delta r$ the transverse field at the midpoint of this bond should be given by $(\phi_A - \phi_B)/\Delta r$ where A and B are the midpoints of the squares 0173 and 0184, respectively (see Fig. 1). This leads to the expression given by Eq. (4) for the transverse field. Swenumson and Thompson[28] chose to express the transverse field at the bond 01 by $(\phi_0 - \phi_4)/\Delta r$. It is apparent that their expression is not symmetric with respect to the segment 01 as it should be. We thus believe that the results of the present work are more reliable. We concur with the conclusion of Swenumson and Thompson[28] that the Hall effect data for Li-NH_3 solutions are compatible with the physical picture of metal-nonmetal transition intermediated by concentration fluctuations.

ACKNOWLEDGMENT

We are grateful to Professor J. C. Thompson for communicating to us the results of his work prior to publication.

---

*Based on research supported by the U. S.-Israel Binational Science Foundation at the University of Tel-Aviv and by the L. Block Fund, NSF Grant No. DMR75-13343, and the Materials Research Laboratory of the NSF at The University of Chicago.

[1]M. H. Cohen and J. Jortner, Phys. Rev. Lett. 30, 699 (1973).
[2]M. H. Cohen and J. Jortner, Phys. Rev. A 10, 978 (1974).
[3]J. Jortner and M. H. Cohen, J. Chem. Phys. 58, 5170 (1973); J. Jortner and M. H. Cohen, Phys. Rev. B (to be published).
[4]M. H. Cohen and J. Jortner, *Proceedings of the Fifth International Conference on Amorphous and Liquid Semiconductors, Garmisch* (Taylor and Francis, London, 1974), p. 167.
[5]M. H. Cohen and J. Jortner, J. Phys. (Paris) 35, C4-345 (1974).
[6]M. H. Cohen and J. Jortner, Amorphous and Liquid Metals, edited by J. Keller (University of Mexico Press, Mexico City, to be published).
[7]I. Webman, J. Jortner, and M. H. Cohen, Phys. Rev. B 13, 713 (1976).
[8]M. H. Cohen and J. Jortner, Phys. Rev. Lett. 30, 696 (1973).
[9]I. Webman, J. Jortner, and M. H. Cohen, Phys. Rev. B 11, 2885 (1975).
[10]I. Webman, M. H. Cohen, and J. Jortner (unpublished).
[11]S. Kirkpatrick, Phys. Rev. Lett. 27, 1722 (1971).
[12]S. Kirkpatrick, Rev. Mod. Phys. 45, 574 (1973).
[13]H. L. Stone, SIAM J. Numer. Anal. 5, 530 (1968).
[14]*Metal-Ammonia Solutions*, edited by J. J. Lagowski and M. J. Sienko (Buttersworth, London, 1970).
[15]*Electrons in Fluids*, edited by J. Jortner and N. R. Kestner (Springer-Verlag, Heidelberg, 1973).
[16]M. H. Cohen and J. C. Thompson, Adv. Phys. 17, 857 (1968).
[17]H. R. Shanks, P. H. Sidles, and G. C. Danielson, Adv. Chem. Series 39, 237 (1963).
[18]K. Ichikawa and J. C. Thompson, J. Chem. Phys. 59, 1680 (1973).
[19]P. W. Schmidt, J. Chem. Phys. 27, 23 (1967).
[20]P. Chieux, Phys. Lett. A 48, 493 (1974).
[21] D. S. Kyser and J. C. Thompson, J. Chem. Phys. 42, 3910 (1965).
[22]R. D. Nasby and J. C. Thompson, J. Chem. Phys. 53, 109 (1970).
[23]J. A. Vanderhoff and J. C. Thompson, J. Chem. Phys. 55, 105 (1971).
[24]R. D. Nasby and J. C. Thompson, J. Chem. Phys. 49, 969 (1968).
[25]L. D. Muhlstein and G. C. Danielson, Phys. Rev. 158, 825 (1967).
[26]P. A. Lightsey, Phys. Rev. B 8, 3586 (1973).
[27]D. P. Tunstall, Phys. Rev. B 11, 2821 (1975).
[28]R. D. Swenumson and J. C. Thompson, Phys. Rev. (to be published).